Journal of Power Sources 624 (2024) 235582

Contents lists available at ScienceDirect

Journal of Power Sources

journal homepage: www.elsevier.com/locate/jpowsour

Recyclability study for the next generation of cobalt-free lithium-ion battery systems with C-LNMO, Si/C- LRLO and TiNbO-LNMO active materials via hydrometallurgical route

Thanu Velmurugan [a], Fabian Diaz [a,b,*], Lilian Schwich [a,b], Monika Keutmann [a], Bernd Friedrich [a]

[a] Institute of Process Metallurgy and Metal Recycling IME, RWTH Aachen University, Intzestraße 3, 52056, Aachen, Germany
[b] MIMITech GmbH, Preusweg 98, D-52074, Aachen, Germany

HIGHLIGHTS

- Gelified electrolytes exhibit a higher thermal stability than ionic liquids.
- Ionic liquid electrolytes exhibit lower toxicity during pyrolysis.
- The CO_2 during pyrolysis is directly proportional to the Li Soluble compounds.
- Recycling achieved 65–90 % recovery rates for Ni, Mn, Li, and anode materials.
- TNO Cathode material can be selectively recovered via weak sulfuric acid leaching.

ARTICLE INFO

Keywords:
Cobalt-free batteries
Lithium-ion battery recycling
Pyrolysis
Leaching
Precipitation
Hydrometallurgy

ABSTRACT

The scarcity and uncertain supply of cobalt poses significant challenges for the lithium-ion battery industry. To address this issue, alternative chemistries excluding cobalt have been developed. Despite solving supply issues, these developments raise concerns about recyclability and their impact on current recycling trends.

This study presents a recycling strategy and evaluates its performance for next-generation cobalt-free lithium-ion batteries. It focuses on three prototypes that use innovative cathode materials (titanium niobium oxide, carbon, and silicon/carbon) and electrolyte systems (ionic liquid and gelified). The proposed recycling process includes pyrolysis, mechanical separation, neutral and acid leaching, cementation, and neutralisation for selective metal separation.

The results indicate that gelified electrolytes exhibit greater thermal stability than their liquid counterparts, indicating an effect on the degradation temperature and gas emissions, which are crucial for metal recovery. This study highlights the reduced toxicity of ionic liquid electrolytes and emphasises the need for strict pyrolysis gas handling due to hazardous emissions. High recovery rates (65–90 %) were achieved for nickel, manganese, lithium, and anode components.

With potential for process optimisation to improve the quality of products, this study shows that cobalt-free battery systems can be integrated into existing recycling frameworks with adjustments, supporting progress towards sustainable battery practices.

1. Introduction

Lithium-ion batteries (LIBs) are long-lasting high-energy storage units widely employed in electronic applications such as electric vehicles, computers, mobile phones, and even in the renewable energy sector. With a predicted lifespan of 3–10 years, such batteries generate a large quantity of waste as they are nearing their end-of-life. Approximately 11 million tons of spent LIBs are expected to be discarded by 2030, with only approximately 5 % being recycled [1]. The LIB market is anticipated to reach 129.3 billion $ in value by 2027 [2]. The number of batteries that have been recycled globally is still small, despite the European Union's attempts to recycle them through the implementation of

* Corresponding author. Institute of Process Metallurgy and Metal Recycling IME, RWTH Aachen University, Intzestraße 3, 52056, Aachen, Germany.
E-mail addresses: TVelmurugan@ime-aachen.de (T. Velmurugan), fdiaz@ime-aachen.de (F. Diaz), bfriedrich@ime-aachen.de (B. Friedrich).

https://doi.org/10.1016/j.jpowsour.2024.235582
Received 7 July 2024; Received in revised form 24 September 2024; Accepted 3 October 2024
Available online 11 October 2024

numerous legislations. Furthermore, due to the increasing demand for LIBs, the cost of crucial elemental resources (lithium (Li), nickel (Ni), and cobalt (Co)) is rapidly increasing [3].

Over the last decade, a substantial increase in demand for LIBs has been anticipated. The necessary capacity is projected to escalate from 700 GWh in 2022 to 4.7 TWh by 2030. This surge is predominantly driven by the adoption of electric vehicles (EVs), which are projected to contribute to approximately 4300 GWh of this demand [4]. In addition, LIBs are preferred for both consumer electronics and stationary energy storage due to their high energy density. Despite the potential of LIBs to surpass automobile batteries, challenges persist in their various material chemistries, including their lifespan, cost, and safety [5–8].

The main components of an LIB typically include an anode, cathode, and separator, which are submerged in a liquid electrolyte and enclosed in a body composed of plastic, aluminum (Al), or stainless steel [4]. Among these, the electrode materials (anode and cathode) and electrolytes are two of the most relevant because they determine the storage capacity and cell potential of a battery [5]. The evolution of LIB materials is driven by the need to improve their performance, safety, and cost-effectiveness [6].

The relevance of Co in the cathode chemistry of LIBs is undeniable. However, their scarcity and uncertain supply chain pose significant challenges. With current demand trends, there is an implicit risk of Co supply shortage within the next decade, especially considering the exponential growth in electric vehicle production [7]. The European Union (EU) is projected to require up to five times more Co by 2030 and 15 times more by 2050 for energy storage and electric car batteries, potentially causing supply issues if unaddressed [8]. Co constitutes up to 60 % of the material cost for battery producers. To ensure profitability in these sectors, a consistent supply of reasonably priced Co is imperative [9]. An alternative approach involves identifying substitutes for this critical element [10,11]. This shift offers several advantages. First, it reduces reliance on costly, scarce Co, and mitigates scarcity-related challenges. Secondly, Co-free batteries promote environmental sustainability by circumventing the adverse effects of Co mining and extraction. Finally, the adoption of Co-free battery chemistry streamlines and economises Li-ion battery manufacturing [9,12].

Currently, only a few Co-free LIBS are successfully available in the market. Among these, $LiFePO_4$ (LFP) is notable for its high energy density and cost-effectiveness, making it increasingly adopted by EV battery manufacturers. Moreover, LFPs are known for their thermal stability, which reduces the need for additional thermal management components. Another known system is the $Li_4Ti_5O_{12}$ (LTO), which offers enhanced thermal stability, high rate capability, and good cycle life despite its higher cost, lower cell voltage, and reduced capacity [13,14]. Despite the availability of these commercialised products, research is ongoing to improve Co-free battery systems, primarily to enhance their energy densities and overall performances [13,14]. Recent developments in Co-free LIB systems have mainly focused on improving Ni-rich layered materials, substituting cations, such as Mg^{2+}, Fe^{3+}, Al^{3+}, and Na^{+}, and enhancing the electrochemical performance and safety of Ni-rich cathodes [9,15–17].

In this study, special emphasis is placed on two European projects, CoFBAT (G.A. No. 875126), and Si-DRIVE (G.A. No. 814464), and research alternatives for Co systems. These projects, pointing to the next generation of batteries that are crucial for the EU's energy transition, focus on Co-free high-voltage cathodes, anodes, and recycling aspects. CoFBAT addresses the development of the cathode material $LiNi_{0.42}Mn_{1.58}O_4$ (LNMO), anode materials such as silicon/Carbon (Si/C) composites and $TiNb_2O_7$ (TNO), and gel polymers as the electrolyte media [18]. Si-DRIVE aims to manufacture amorphous silicon-coated anodes using polymer/ionic-liquid electrolytes and sustainable Li-rich high-voltage cathodes. The goal is to enhance energy density, cycle life, fast charging, and safety [19]. Both projects aimed for sustainable and competitive LIB technologies, supporting cleaner energy, effective recycling performance, and enhancing the EU's global market.

Research on new Co-free battery systems will undoubtedly provide substantial advantages to the battery manufacturing sector, including enhanced performance and sustainability [18,19]. However, recycling cobalt-free batteries presents challenges, as current methods are tailored for cobalt-containing batteries. Ensuring sustainability requires understanding the compatibility of new battery systems with existing recycling techniques and developing specialised approaches for recovering valuable materials. The development of effective recycling solutions is crucial for upholding the circular economy and minimising the environmental impacts. In this regard, new Co-free systems will need to comply with the current and upcoming recycling regulations. In this regard, the European Union has strict recycling regulations for LIBs under the Battery Directive (Directive 2006/66/EC) and the Waste Electrical and Electronic Equipment (WEEE) Directive (Directive 2012/19/EU) [20,21]. The newly proposed European guidelines set the collection goals for LIBs at 65 % by 2025 and 70 % by 2030. For LIBs, the recycling targets for material recovery are expected to be 90 % for Ni, 35 % for Li, and 90 % for Cu by 2025 and 95 % for Ni, 70 % for Li, and 95 % for Cu by 2030 [22,23]. These regulations promote sustainability and circular economy for the development of LIBs.

The primary objective of this study is to propose a recycling concept based on the literature, investigating the behaviour of current prototype Co-free systems. This encompasses the evaluation of experimental cathode materials (TNO, Carbon (C), and Si/C) and the utilisation of two different electrolyte systems (liquid and gelified). These materials are expected to represent an important alternative to conventional onces in the next generation of Lithium ion batteries.

This study also assessed the compatibility of the chemistry of battery prototypes with the recycling approach used for commercial batteries. The recycling concept employed a well-known hydrometallurgical approach (based on [18,19]), involving pyrolysis, mechanical separation, neutral leaching, acid leaching with sulfuric acid and hydrogen peroxide as additives, cementation, and neutralisation with sodium hydroxide for selective metal separation.

It is important to clarify that this study should be considered as the first building block for the recycling of selected cobalt-free systems and not as a finalised concept. This is due to the limited amount of prototype material used in the experimental work. However, the controlled utilisation of input materials should contribute to the scientific understanding of material behaviour during recycling. The results should provide a good indication for future perspectives if the selected cell design, or a similar one, reaches the market in the coming years.

This study contributes significantly to advancing recycling practices for Co-free battery systems and promoting sustainable battery development.

2. Background on the recycling concept for the Co-free batteries

To develop efficient recycling strategies for new battery systems, it is crucial to explore existing recycling methods compatible with their material chemistry. Various established procedures are available in the recycling sector that are tailored to specific systems and target metals for recovery. Typically, the recycling process involves dismantling, followed by thermal or mechanical pre-processing, mechanical separation, and extraction methods [24,25]. In this study, emphasis was placed on pyrolysis as a pretreatment method to handle hazardous halogenated electrolytes and hydrometallurgical processing for metal extraction, which consisted of neutral leaching, acid leaching, cementation, and controlled precipitation steps. This approach has been highlighted for its advantageous selective operation in terms of metal recovery and safety, particularly when compared to pyrometallurgical extraction methods [26].

Pyrolysis is defined as the thermal degradation of organic compounds at high temperatures in a controlled setting, in the absence of oxygen. The heating temperature in pyrolysis technology must be carefully chosen to successfully degrade most organics, binders, and

electrolytes. These materials often hinder the efficiency of hydrometallurgical extraction methods [34]. Moreover, transition from insoluble Li compounds to more soluble species can be achieved via Li carbonisation [27]. After pyrolysis, the separation of metals from the black mass in the metallic form occurs mechanically via crushing and sieving [24]. In this context, black mass refers to the fine nonmetallic residue containing the majority of the anode and cathode materials after the metals are separated from the rest of the battery residue. The fine black powder contained the majority of the elements targeted for extraction [26].

Later, neutral leaching of the black mass takes place, allowing early extraction of Li in the recycling chain. Neutral leaching uses water to selectively extract Li from the black mass. This process targets water-soluble Li compounds. In contrast, leaching of manganese (Mn), Co, and Ni under these conditions is avoided [28]. After filtration, the delithiated black mass follows the next process step, while Li is extracted from the pregnant solution via precipitation [29].

Different references can be found aiming to select the "correct" solid: liquid ratio and temperature to extract Li in netral leaching. One study found that at a solid-liquid (S:L) ratio of 25 g/L, water leaching led to the dissolution of approximately 83 % of Li. In a separate study, it was found that 93 % of Li could be leached and recovered as Li_2CO_3 when the pyrolysis samples were leached three times at an S:L ratio of 50 g/L [29]. The efficiency can be affected by the process temperature; for instance, Li leaching was notably high at 93 % when carried out at 25 °C, but decreased to 79 % at 80 °C. This decrease is attributed to the reduced solubility of Li_2CO_3 at higher temperatures. Therefore, it is recommended that a water leaching operation be conducted at room temperature [30].

After neutral leaching, the delithiated black mass was subjected to acid leaching for metal extraction. However, determining the parameters for recycling feasibility studies is challenging because of limited prior research on the discussed Co-free battery chemistries. Nevertheless, acidic hydrometallurgical extraction methods for other chemistries are well-documented and may be compatible, except for cases involving cobalt and commercial electrolytes.

Current studies have explored both organic and inorganic acids to leach cathode substances for extracting important metals, such as Ni, Mn, and Co. Inorganic acids, such as phosphoric acid (H_3PO_4), sulfuric acid (H_2SO_4), nitric acid (HNO_3), and hydrochloric acid (HCl) are used in the leaching process [28,31]. Additionally, reducing agents such as hydrogen peroxide (H_2O_2), sodium bisulfite, or glucose are employed to convert the high-valence states of Co or Mn into easily soluble forms such as Co^{2+} and Mn^{2+}, while leaving Li as Li^+ ions without undergoing reduction [32]. To enhance efficiency, H_2SO_4 is commonly used in conjunction with reducing agents [33]. Table 1 compiles significant publications that employed H_2SO_4 as the leaching medium under various parameters, achieving notable recovery rates. This information is pertinent for establishing a foundation for the leaching concept in Co-free batteries in this study.

The process of recovering valuable metals from the leached materials follows a systematic approach. Initially, Cu is separated from the leached solution in a process known as Cu cementation using Fe because it effectively reduces the presence of noble metal ions [34].

Once Cu is extracted, Al and iron (Fe) takes place through metal hydroxide precipitation, followed by the precipitation of Ni, Mn, and Co. pH is a critical factor in this process. If the pH is too low, the complete removal of Al and Fe may not be achieved. Conversely, at high pH, there is a risk of the co-precipitation of Ni and Mn [35,36].

Maintaining an appropriate pH value is essential to maximise the removal of Fe and Al, while minimising the loss of other valuable elements. The reported results indicated that at an equilibrium pH of 3.3, over 99 % of Fe(III) and 62 % of Al(III) were successfully extracted, whereas only 1.1 % of Ni, Mn, and Li were lost [37,38].

Finally, by adjusting the pH to reach 11, where Ni precipitates at pH 9 and Mn at pH 10.4, the remaining cathode metal is precipitated. Subsequently, crystallisation of Li_2CO_3 occurs through titration with Na_2CO_3 in the presence of the remaining alkaline solution, resulting in the formation of Li crystals [34].

As the industry shifts towards cobalt-free batteries, there remains a critical gap in understanding the optimal recycling processes for these emerging battery systems. This study fills that gap by introducing the prototype systems in stablished methodologies, enhancing the recovery efficiency of key metals like lithium, nickel, manganese, titanium, niobium and graphite. The insights gained from this research have the potential to significantly influence future recycling practices and battery design, ensuring that the transition away from cobalt is both efficient and environmentally responsible.

Table 1
Summarises recent scientific studies on acid leaching for LIBs recycling.

Battery system[a]	Media (Mol H_2SO_4) - Additive	Temp (°C)	S/L ratio (g/L)	Time (h)	Recovery method	Best Efficiency achieved (%)	REF
NMC	3,5 M	85	1:5	3	Evaporative Crysystallization, Solvent extraction	Li-85, Ni-98, Mn-99	[39]
	3 M	80	1:15	1	precipitation	Li-99, Co-99	[40]
	2 M − H_2O_2	80	1:0.05	1	selective precipitation, solvent extraction	Li-99, Ni-98, Co-98	[36]
	4M	60	1:0.03	2	–	Li-94, Ni-93, Co-98, Mn-99	[41]
	2 M −H_2O_2	50–80	1:10,1:30,1:50	1	Solvent extraction	Li-95, Co-80	[42]
NCA	3 M	50–90	1:15	5	Solvent extraction	Co-94, Ni-94, Cu-94	[43]
	2 M	25–90	1:20	3	precipitation	Li-78, Ni-38, Co-42, Al-36	[44]
	4 M	80	1:5	1	Leachant	Ni-82, Co-80, Al-30	[45]
LCO	2 M − H_2O_2	60	1:33	2	precipitation	Co-96, Li-88	[46]
	2 M − H_2O_2	75	1:10	1	Solvent extraction	Li-94, Co-93	[47]
	2 M − H_2O_2	60	1:10	2	Solvent extraction	Co-99, Li-99	[48]
	2 M −H_2O_2	75	1:20	1	–	Co-80, Li-100	[49]
	2 M − H_2O_2	80	1:20	1	Leachant	Li-99	[50]
LTO	4 M − H_2O_2	80	1:40	4	Solvent extraction	Li-97, Ti-98	[51]
LMO	2 M	25	–	1/2	Solvent extraction	Mn-85	[52]
LFP	0.3 M − H_2O_2	25–80	1:100	2	precipitation	Li-99, Fe-78,	[53]
	2 M	60	1:20	2	Leachant	Li-96, Fe-93	[54]
	0.2 M -H_2O_2	60	1:100	2	Solvent extraction	Li-96, Fe-5	[35]

[a] NMC- Lithium Nickel Manganese Cobalt Oxide, NCA- Lithium Nickel Cobalt Aluminum Oxide, LCO - Lithium Cobalt Oxide, LMO - Lithium Manganese Oxide, LTO - Lithium Titanate, LFP- Lithium Iron Phosphate.

3. Material and methods

3.1. Materials

The raw materials utilized in this study were based on the baseline design of three prototype batteries, which are integral to the ongoing development of two European projects: Si-drive and CoFBAT. These prototypes represented a relatively advanced design. Although variations in the final cell composition might occur in these ongoing projects, they do not affect the fundamental knowledge generated in this study.

The first system, referred to as the C-LNMO System, consisted of an anode made of graphite and a cathode composed of LNMO ($Li_{1.0}Ni_{0.42}Mn_{1.58}O_4$ -Lithium Nickel Manganese Oxide). Cu and Al foils were used as current collectors in the battery system. Polyvinylidene fluoride (PVDF) served as a binder material to maintain the electrode integrity. Graphite was used in both the anode and cathode materials, with an additional C65 material. The electrolyte used in this system was a gelified electrolyte, which was a Gel Polymer Electrolyte (GPE) developed in CoFBAT and described as a crosslinked PVDF based membrane. The baseline of the used electrolyte for the full cell consisted 227 of Celgard 2500 (25 μm thick) + 100 μL of liquid electrolyte 1M LiPF6 ethylene 228 carbonate (EC):dimethyl carbonate (DMC) (1:1 vol) (LP30) and 3 wt % FEC. In this 229 system, an Fe-based metal casing was employed in the commercial format 21700.

The second system, known as the TNO-LNMO System, is comprised of an anode made of TiNbO ($TiNb_2O_7$ - Titanium Niobium Oxide) and a cathode composed of LNMO. The Al foil was the only current collector in this system, and the metal casing was composed of Fe. C65 graphite and PVDF were used in these systems. The electrolyte used was the same Gelified Electrolyte used in the first system.

The third system, labelled the Si/C-LRLO System, features an anode made of Si/C-coating (silicon/carbon-coating) and a cathode composed of lithium-rich layered oxides (LRLO). Cu and Al foils were employed as the current collectors and tabs, respectively, in this battery system with an Fe metal casing. This system utilises a liquid electrolyte containing an ionic liquid electrolyte known as LiFSI:EMIMFSI. The ionic liquid electrolyte EMIMFSI has the chemical formula $LiC_2NO_4F_6S_2$: $C_6H_{11}F_2N_3O_4S_2$.

In this study, PVDF was used as a binder in the first two systems. However, the Si/C-LRLO system did not include PVDF in its design, as the physical properties and supporting feature of the ionic liquid, silicon/carbon-coating, and ceramic layers allow for manufacturing of the batteries without the explicit use of such a binder.

Because of the sensitive data regarding the intellectual property associated with the design of the batteries and the experimental electrolyte materials used in this study, we cannot provide a detailed material distribution of the input materials. For more information about their design and development, please refer to official project websites [55,56].

3.2. Experimental

The experimental strategy proposed in this study for recovering valuable metals from Co-free batteries is shown in Fig. 1. This flow chart shows the techniques, additives, and end-products required for the separation of metals.

In the following sections, information related to the parameters and experimental procedures is addressed in detail for each process step. In this study, each of the three systems underwent two sets of trials.

3.2.1. Pyrolysis

The tests were conducted in a programmed resistance furnace using

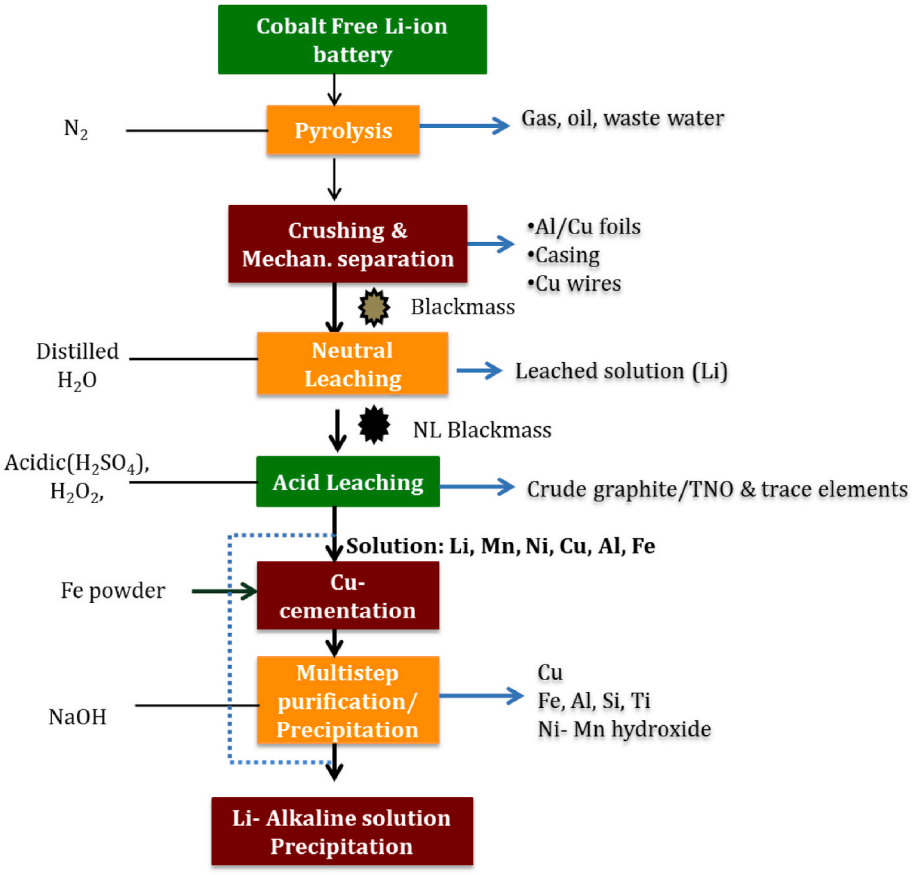

Fig. 1. Proposed method for recycling Co-Free Batteries.

the stationary pyrolysis method. To create a closed environment, a 1-litre volume reactor was utilized, which was sealed with a water-cooling lid. The top features of the reactor include a pressure gauge, thermocouple, carrier gas input, gas-sampling vent, and exhaust (Fig. 2). Additionally, a Fourier Transform Infrared spectrophotometre (FTIR) system was connected to the outside valve of the reactor to measure and analyse the gases produced during the reaction, which is crucial for understanding the degradation of organics and assessing environmental safety.

FTIR allows the measurement of gaseous components, such as H_2O, CO_2, CO, HF, and other volatile organic compounds (VOCs). The gas inlet (N_2) was connected to the top of the reactor and the exhaust was directed to the scrubber. The scrubber consisted of two bottles: one containing alkaline to clean the off-gas and prevent oxygen backflow into the reactor, and the other serving as a safety measure to prevent water ingress from the second bottle into the reactor in the case of a pressure drop inside. The pyrolysis process began by charging 162.5 g of the synthetic battery formulation into the reactor using a crucible. The reactor was closed and placed in a furnace. Nitrogen gas was introduced into the reactor from the top at a rate of 6 l/min to drive the pyrolytic gas created during the process into the hot tube, thereby preventing the subsequent pyrolysis reactions. The furnace was heated at a constant rate of 350 °C/h, until the temperature reached 600 °C. Once the desired temperature was reached, the reactor was maintained at this temperature for 2 h and then cooled.

3.2.2. Crushing and mechanical separation

After pyrolysis, the pyrolysed material was ground to separate black matter from the metallic components. A benchtop ball-milling machine was used for 10 min at 500 rpm. The milling process involved mixed-size grinding balls (10–30 mm) weighing 0.75 kg per set. The milled material was sieved. Different sieves measuring 5, 2, and 1 mm were used to separate the coarse and metallic particles from the powder. In this step, the coarse fraction (>2 mm) of metallic materials such as Cu, Al, and casings was separated. Following mechanical separation, the black mass (<1 mm) was advanced to the subsequent leaching step, and a sample was collected for chemical analysis. Residual metal foils were weighed to calculate the mass balance.

3.2.3. Neutral leaching

The traditional hydrometallurgical process was selected for this battery system recyling due to its superior recovery efficiency, cost-effectiveness, and environmental benefits as the result of relatively weak acids and abundant reagents. It enables high-purity extraction of lithium, nickel, and manganese while consuming less energy than alternative methods. Additionally, its versatility across different battery chemistries makes it particularly effective for the recycling goals of this study.

Following the separation of the fine black powder, the black mass was placed in a 2000 ml glass beaker with deionised water at a 1:40 ratio. The mixture was stirred at room temperature for 2 h at 300 rpm using a magnetic stirrer. Filtration was conducted using a funnel and filter paper with the aid of a vacuum pump. This filtration technique was employed in all solid-liquid separations in the following steps. The filtered material was dried in an oven, and its weight was measured. Additionally, a small sample of the leached solution and dried black mass were retained for analysis.

3.2.4. Acid leaching

The dried delithiated black mass was weighed after neutral leaching and transferred to a 1000 ml beaker for acid leaching. At an ambient temperature of 80 °C, the weighed black mass was dissolved in 2.5 M H_2SO_4 at a ratio of 1:10 for 2 h while being continuously mixed at a speed of 300 rpm and heated with the help of a heating plate. Thermal probes were used to monitor and regulate the temperature. Subsequently, the leaching process was followed by filtering. The solution was then used for additional precipitation stages, and samples were collected for analysis. The leached black mass was then dried and stored for analysis.

3.2.5. Cementation step

The pregnant solution from the acid leaching was used for the Cu cementation process. The solution was heated to 60 °C and stirred at 300 rpm. pH control is essential for the removal of Cu from the solution. NaOH solution (100 ml) (300 g/l concentration) was added dropwise until the pH reached 1.15. Then, 19.65 g/l of $CuSO_4$ and 7.5 g/l Fe powder were added to the solution. $CuSO_4$ was introduced following the recommendations of previous studies [57]. This step was performed for

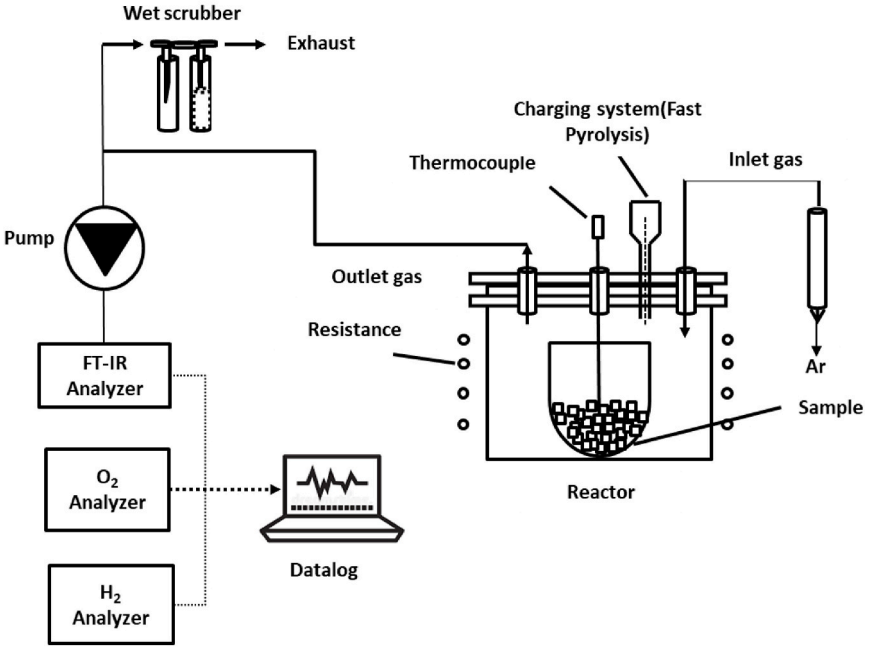

Fig. 2. Experimental setup for slow Pyrolysis of battery products.

30 min. Filtration was then performed to separate and dry the Cu cementates, and a sample of the solution was retained for the analysis.

3.2.6. Fe-Al precipitation

After removing the Cu, the remaining solution was heated to 60 °C and stirred at 300 rpm. NaOH solution (150 ml) (300 g/l concentration) was added dropwise until the pH concentration reaches 2.6–2.8. Then, 13.33 ml of H_2O_2 was added as the oxidising agent. NaOH (70 ml) was then added to increase the pH to 3.3. Once the required pH level was reached, the solution was filtered to separate the Al-Fe hydroxide cake and the samples were stored for analysis.

3.2.7. Cathode metal precipitation

In this step, the solution was maintained at room temperature, only stirring was required, and NaOH (80 ml) (300 g/l concentration) was gradually added to the solution until the pH reached 10. The solution turned into a slurry owing to the precipitation of metals, which was then filtered. The filter cake was dried and stored for chemical analysis. The remaining alkaline solution was collected for further characterisation.

3.3. Analytical methods of the hydrometallurgical products

Spectro ICP-OES (Spectro CIROS Vision, Spectro Analytical Instruments GmbH) is used for analyzing the liquid samples and filter cakes after acidic dissolution (HNO_3). The Li and fluoride contents were measured using an Ion-Selective Electrode (METTLER TOLEDO). The combustion methods for carbon and sulfur analysis (ELTRA CS 2000, ELTRA GmbH) and fluoride analysis (A1 Combustion-IC) were used to identify the black mass composition.

3.4. Determination of elemental efficiency and total efficiency of the recycling concept

Following the chemical analysis, the following formula was used to determine the metal recovery efficiency:

$$\eta_a = \frac{m_{a,i}}{M_{a,T}} * 100\%$$

where η_a is the elemental efficiency of a metal a, $m_{a,i}$ is the mass of a metal a in a targeted product i and $M_{a,T}$ represents the total mass of metal a found in the studied battery system, measured in the input material.

The total recycling efficiency is defined as the sum of all the metals recovered over the weight of the input battery system in terms of weight percentage.

4. Results and discussion

The difference in the electrolyte material was carefully evaluated, as both gelified electrolytes and ionic liquid electrolytes are experimental materials for next-generation batteries. Degradation of these materials during pyrolysis is discussed in the following section. Subsequently, a thorough discussion of the recycling performance of the individual components in each process step is provided.

4.1. Volatile material behavior during pyrolysis: gelified vs ionic liquid electrolyte

The evaluation of the off-gas composition during pyrolysis of the gelifed presented in C-LNMO and TNO-LNMO, and liquid electrolytes presented in Si/C-LRLO, indicated different patterns while heating the material.

Fig. 3 shows that, in general, the ionic liquid electrolyte showed a

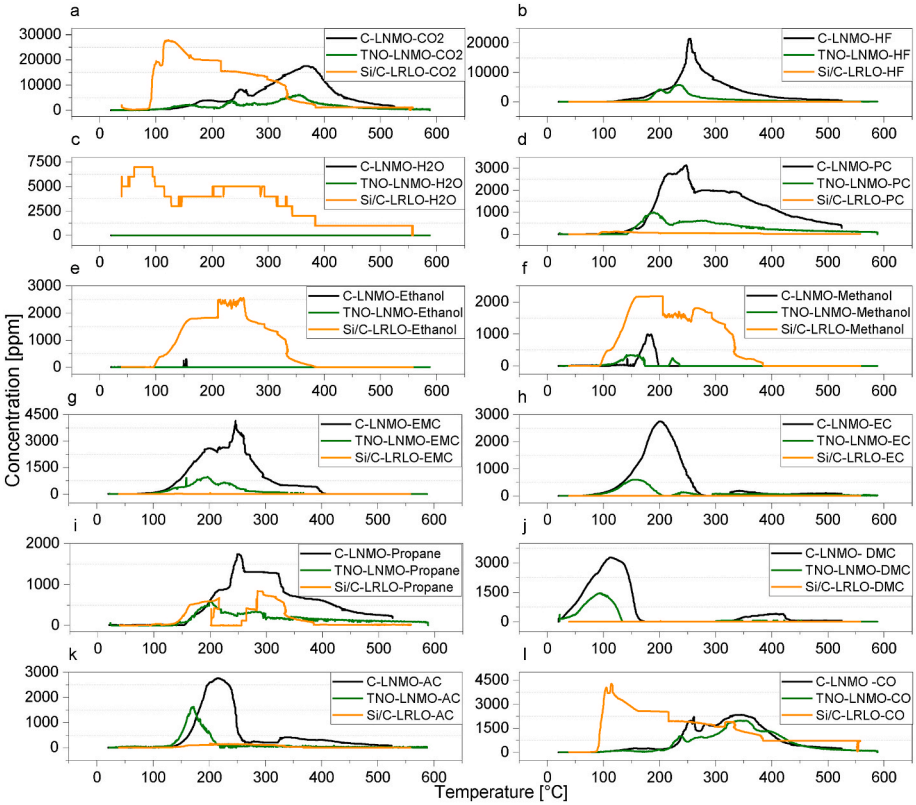

Fig. 3. FTIR results of gas emission during pyrolysis applied to (a)Carbon dioxide, (b) Hydrogen fluoride, (c) Water vapor, (d) Propylene carbonate, (e) ethanol, (f) methanol (g) Ethyl methyl carbonate, (h) Ethylene carbonate, (i)Propane, (j) Dimethyl carbonate, (k) Acetaldehyde, (i) Carbon monoxide.

more unstable condition at lower temperatures, above 100 °C, compared to that of the gelified material. For the ionic electrolyte, the initial step of the process involved a drying phase between 70 °C and 100 °C, during which dehydration occurred. This was verified by the identification of H_2O gas. This compound was further in temperature registered but was most likely a product of the degradation of organic matter. In addition, a second phenomenon can also be identified at 100 °C, which is characterised by a redox reaction where gases such as CO_2 and CO are formed alongside organic gases such as methanol, ethanol, and propane. This stage involves reactions between the hydrocarbons and CO_2 gases [58].

CH_3OH (methanol) generated in both studied electrolytes was generated at temperatures between 100 and 400 °C as a primary product in low-temperature reactions involving DMC and ethyl methyl carbonate (EMC) [59].

In the case of the gelified electrolyte, the two systems showed little difference, except for an increased degradation yield in C-LNMO, marked by gases in increased concentration, despite the same amount of electrolyte in the studied material, compared to that of TNO-LNMO. In contrast to the ionic liquid electrolyte, H_2O vapor was not observed in this electrolyte over the entire temperature range. Moreover, the off-gas was characterised by the early volatilisation of electrolyte solvents such as EC and DMC at low temperatures, even below 100 °C, followed by PC at approximately 150 °C in the resulting gas. The difference between the two systems could be attributed to the catalytic effect of graphite in the samples [60]. Based on these results, it is evident that the gelified polymer degraded to form organic gases such as propane, acetaldehyde, and propylene carbonate.

During this process, certain organic compounds within the battery, including the electrolyte, can decompose, generating gases, such as propane. Both systems with gelified electrolytes also produced organic gases, such as DMC, EMC, and EC, because of the decomposition of the $LiPF_6$ gel electrolyte. Conversely, H_2O, ethanol, and methanol were observed only in the Si/C-LRLO system. EC evaporation was observed over a wide temperature range, spanning from 100 °C to 270 °C, with a distinct peak at 200 °C. Nonetheless, in the presence of a certain amount of Li, a minor fraction of EC underwent decomposition, resulting in the formation of CO_2, as shown in equation (1) [61].

$$2Li + 2EC \rightarrow Li - O - (CH_2)_4 - O - Li + 2CO_2 \quad (1)$$

In all three systems, CO_2 and CO were predominant gases. However, in the ionic liquid electrolyte system, they are generated at much lower temperatures (below 100 °C) and progressively decrease in formation after peaking at approximately 125 °C until reaching 400 °C. Conversely, gelified electrolytes (C-LNMO and TNO-LNMO) exhibit different behaviours. Specifically, the graphite-containing material released higher concentrations of CO_2, CO, and other hydrocarbons than TNO-LNMO. In both cases, these gases were produced during the degradation of the gelified electrolyte and only occurred after 200 °C, with two peaks of generation at approximately 250 °C and 350 °C, respectively. In all three systems, CO_2 and CO were barely detected at temperatures above 400 °C.

The generation of gases such as CO_2 and CO can be expected through thermal degradation during pyrolysis due to the presence of compounds within the hydroxyl (• OH) functional group [62]. These substances undergo thermal breakdown when heated to high temperatures, producing a variety of by-products including free OH radicals [58]. These free OH radicals are the main sources of oxygen in oxidative reactions, leading to the formation of CO and CO_2, as shown in equation (2) [58]. The presence of hydroxyl radicals was evidenced in the registered methanol in all the studied systems and ethanol, especially in the ionic electrolyte.

$$CO + \bullet OH = CO_2 + H \quad (2)$$

The generated OH radicals could also form water (H_2O) molecules. This is a simplified representation, as CH_3 could potentially react with •OH to form CH_3O; however, these processes involving methyl are not significant throughout pyrolysis. One sub-mechanism leads to the production of CO, and the other results in the generation of hydrocarbons and H_2O [58].

The OH radicals could also be generated from methanol during pyrolysis, as detected by FTIR, as shown in equations (3) and (4) [63].

$$CH_3OH + M \rightarrow \bullet CH_3 + \bullet OH + M \quad (3)$$

$$CH_3OH + M \rightarrow \bullet CH_3O + H + M \quad (4)$$

The reverse reaction involving CH_3 is also a critical factor for CO_2 consumption. In this process, methoxy radicals (CH_3O), such as methanol and CO, can be generated, as shown in equation (5) [64].

$$\bullet CH_3O + CO \leftrightarrow \bullet CH_3 + CO_2 \quad (5)$$

Nevertheless, the oxidation pathway that resulted in the formation of CH_3O was facilitated as the concentrations of O and •OH in the mixture increased. This leads to the accelerated production of CO, particularly with increasing CO_2 fraction [63].

The initiation of pyrolysis is believed to have an impact on the unimolecular decomposition of ethanol, which is formed above 100 °C with the ionic electrolyte and small traces in the gelified electrolyte. If this is indeed the case, this implies the existence of a reaction that produces hydroxyl radicals, as shown in equation (6) [65].

$$C_2H_5OH \rightarrow \bullet C_2H_5 + \bullet OH \quad (6)$$

When examining the pathways for CO_2 consumption in both types of electrolytes for these hydrocarbons, it is clear that the CO_2 reaction taking the right path (involving H, singlet methylene, and methyl) predominates significantly during propane formation, as shown in equation (7) [64]:

$$C_3H_8(+M) \leftrightarrow \bullet C_2H_5 + \bullet CH_3 + CO_2 \quad (7)$$

These reactions (equations (3), (4) and (6)) involve both the formation and decomposition of unsaturated hydrocarbons, and significantly affect the consumption of H radicals. Consequently, they could play a substantial role in the utilisation of CO_2 and concurrent generation of CO [64].

Pyrolysis is a complex process that involves multiple simultaneous reactions. For instance, in addition to the cracking of organics, the reduction reactions of metal oxides can lead to CO and CO_2 formation during pyrolysis [58]. In the context of LIB pyrolysis, for all three systems, some anticipated reactions in the pyrolysis process concerning Li-containing compounds could occur, as shown in equations 8–11 [66,67]:

$$Li_2O_{(s)} + CO_{2(g)} \rightarrow Li_2CO_{3(s)} \quad (8)$$

$$Li_2O + 2HF \rightarrow 2\,LiF + H_2O \quad (9)$$

$$Li_2CO_3 + 2HF \rightarrow 2\,LiF + H_2O + CO_2 \quad (10)$$

$$Li_2O_{(s)} + H_2O_{(g)} \rightarrow LiOH \quad (11)$$

According to Equations, in systems involving C-LNMO, TNO-LNMO, and Si/C-LRLO, both LNMO (Lithium Nickel Manganese Oxide) and LRLO (Lithium-Rich Layered Oxide) materials, which can include $LiMn_2O_4$ and $LiNiO_2$ as part of LNMO and LRLO, are expected to experience reactions that lead to the generation of reducing gases and changes in the forms of metallic components or oxides with lower oxidation states. $LiMn_2O_4$ can be transformed to Mn_3O_4, Li_2CO_3, Li_2O, MnO, CO, and CO_2. Similarly, as indicated in equations 12–15 [66], $LiNiO_2$ can be transformed into Ni, Li_2CO_3, Li_2O, NiO, CO, and CO_2

$$2.4\,LiMn_2O_{4(s)} + C_{(s)} \rightarrow 1.2\,Li_2O_{(s)} + 1.6\,Mn_3O_{4(s)} + CO_{2(g)} \quad (12)$$

$$3\,LiMn_2O_{4(s)} + 2.5CO_{(g)} \rightarrow 2\,Mn_3O_{4(s)} + 1.5\,Li_2CO_{3(s)} + CO_{2(g)} \quad (13)$$

$$4\,LiNiO_{2(s)} + C_{(s)} \rightarrow 2\,Li_2O_{(s)} + 4NiO_{(s)} + CO_{2(g)} \quad (14)$$

$$2\,LiNiO_{2(s)} + 3C_{(s)} \rightarrow Li_2O_{(s)} + 2Ni_{(s)} + 3\,CO_{(g)} \quad (15)$$

Another important observation in Fig. 3 is related to the formation of HF during the pyrolysis. As can be seen, this component also exhibits a significant difference when using gelified electrolyte compared to ionic liquid electrolyte. HF showed a gradual increase above 100 °C for the system with graphite as the cathode material, and only above 170 °C for the system with TNO. In both systems, the HF formation peak was reached at approximately 250 °C, with increased formation in the C-LNMO system. Experiments using an ionic liquid electrolyte did not indicate the formation of HF over the entire experimental temperature range. This behaviour could be attributed to the presence of PVDF in both systems using a gelified electrolyte, which led to the release of gases, such as CO and HF, along with the formation of solid carbon residues. PVDF decomposes at temperatures between 250 and 500 °C, depending on the rate, pressure, and dwelling time, as shown in equation (16) [68]. The HF gas release in the Si/C-LRLO system was low because of the absence of PVDF as a raw material.

The pyrolysis of PVDF results in:

$$-(C_2H_2F_2)_n - \rightarrow (C_xH_yF_z) + HF_{(g)} + C \quad (16)$$

Lithium fluoride (LiF) may occasionally be created when HF reacts with lithium hydroxide (LiOH) in a battery to form LiF, as indicated in equation (17) [69].

$$HF + Li^+ + \bullet OH^- = LiF + H_2O \quad (17)$$

Notably, LiF is typically an undesired compound because of its low solubility in water [70], which could pose challenges in the subsequent neutral leaching steps.

The release of pyrolysis gas stopped after a certain time at a higher temperature. The release of gas during pyrolysis in the liquid ionic electrolyte system decreased after reaching 400 °C to almost zero, whereas in the gelified electrolyte systems, the release was the same after reaching 450 °C and 500 °C for TNO-LNMO and C-LNMO, respectively. As a result, there was no gas emission from pyrolysis after a given period of time, indicating that the chemical reaction inside the pyrolysis was complete.

When comparing the gases released from the three systems, CO_2 emissions were the highest, followed by HF, CO, and other organic gases. Because of its electrolyte and battery system, Si/C-LRLO with an ionic liquid electrolyte exhibited the lowest levels of harmful gases because it had lower HF gas emissions, which are more toxic than other gases such as CO_2 and CO [58].

Although considerable attention has been directed towards investigating the off-gases generated by LIBs, no special method has been proposed to quantitatively assess the overall toxicity of these off-gases. To address this, the USA's Protective Action Criteria (PAC) were introduced for battery pyrolysis to allow for a quantitative comparison of off-gas toxicity [58]. PAC_1 represents the mildest toxic hazard of a substance. Essentially, it is used to calculate the theoretical contaminated volume of a single LIB, which is subsequently used to evaluate its toxicity.

The theoretical contaminated volume of a single LIB can be described as the cumulative volume necessary to ensure human health safety for all substances identified in an off-gas environment. The toxicity value is calculated by the following formula shown in equation (18).

$$V_{contaminated} = \sum \frac{V_{substance}}{PAC_1} \quad (18)$$

where $V_{contaminated}$ represents the total contaminated volume of space based on toxicity value of all specific component in the off-gas. $V_{substance}$ denotes the volume or concentration of each individual substance present in the off-gas. PAC1 is a parameter known as the "Pollutant Abatement Coefficient," which normalizes the concentration values to account for their relative toxicities.

The total volume per component of gas produced during pyrolysis is calculated by integrating the time-concentration records from FTIR, obtaining the total volumes in Liters, as shown in equation equation (19). Where V is the volume of compound (Liter), d is the diluted ratio of the FTIR, $\dot{V}$ is the flow rate of carried gas (L/min), c_i is the concentration of compound at time t_i (ppm), c_{i+1} is the concentration of compound at time t_{i+1} (ppm).

$$V = \frac{1}{d}\sum_{i=0}^{n} \dot{V}(t_{i+1} - t_i)(c_{i+1} + t_i) \Big/ 2 \quad (19)$$

In essence, the greater the theoretical contaminated volume, the more toxic is the off-gas considered [58]. Fig. 4 shows the calculated toxicity released during the pyrolysis of the three systems with both the ionic liquid and gelified electrolyte.

Among the different systems, the C-LNMO system with a gelified electrolyte, utilising graphite as its anode material, produces the highest quantity of harmful gases, particularly HF and PC gas, which are notably more toxic than those produced in TNO-LNMO with the same electrolyte and Si/C-LRLO with the ionic liquid electrolyte. Propylene Carbonate is another significant contributor to toxicity in all systems, and is the main source of toxicity for the ionic liquid electrolyte, with smaller amounts of Dimethyl Carbonate and Ethylene Carbonate. In this regard, TNO-LNMO was ranked as having the second-highest registered toxicity. The system with the lowest toxicity registered corresponds to the Si/C-LRLO system with the ionic liquid electrolyte, which emits the lowest total volume of gases but still contains PC and HF gases as pollutants. Indeed, it is relevant to treat pyrolysis gases not only to safeguard the environment but also to ensure compliance with safety regulations.

The pyrolysis gases can undergo treatment processes involving scrubbers, amine solvent absorption equipment, and membranes to mitigate their toxicity; in some cases, certain gases can be transformed into valuable products.

4.2. Metal dispersion and recycling efficiency through the recycling process

During neutral leaching, the effects of pyrolysis were discernible. Depending on the pyrolysis process state and the studied material, the early Li recovery showed a distinct trend. High temperatures can

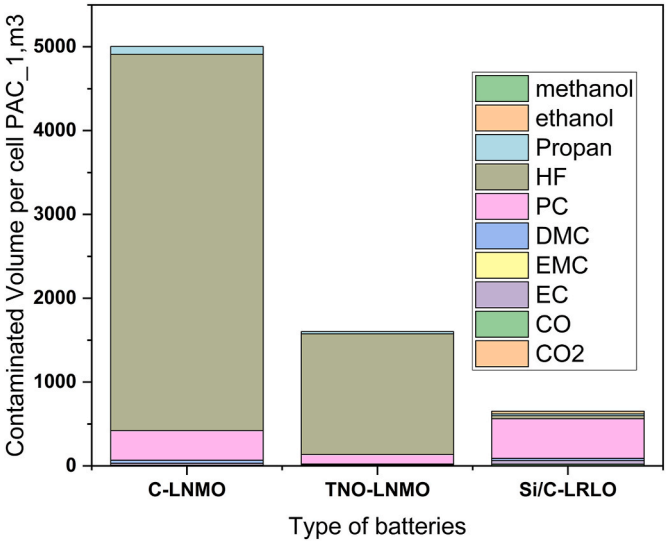

Fig. 4. Theoretical contaminated volumes for individual substances of three different battery system during pyrolysis.

promote Li to become more reactive, leading to the formation of lithium oxide (Li_2O) or lithium carbonate (Li_2CO_3) during the consumption of CO_2 [66]. Due to the possibility that CO_2 may react with LiOH to make Li_2CO_3.

For neutral leaching, favouring compounds that are more soluble than others is necessary to achieve a higher Li yield in the process. Therefore, the formation of Li_2O (1.3 g/L) and LiF (1.14 g/L) is less desirable than that of Li_2CO_3 (13 g/L) and LiOH (130 g/L) [70–72].

As shown in Fig. 5, a linear correlation existed between Li leaching in water and the quantity of CO_2 generated during pyrolysis. Based on Fig. 5 and the understanding that oxygen is not present during pyrolysis in gas form, it can be said that CO_2 formation can be mostly attributed to reduction reactions involving Li species, thus leading to the formation of soluble compounds such as carbonates in the black mass during the pyrolysis process. In addition, the significant interaction of CO_2 with other compounds at high temperatures could also be a driving force for the carbonisation of Li at high temperatures [73].

In the results shown in Fig. 5, when comparing the studied materials, the Si/C-LRLO system exhibited the highest Li recovery and CO_2 emissions. In contrast, the TNO-LNMO system exhibited the lowest Li recovery, which corresponded to its lower CO_2 emissions. This implies that carbon-containing matter, either as an ionic liquid, gelified electrolyte, or graphite, plays a crucial role in the efficiency of early Li extraction. As previously discussed, in the context of pyrolysis, the TNO-LNMO system exhibits the lowest organic-containing material and most probably leads to a greater LiF content compared to the other systems. This, in turn, resulted in reduced Li leaching during the subsequent neutral leaching processes.

The neutral leaching results, except for the TNO-LNMO system, indicate competitive performance compared to existing commercial battery systems containing Co, where the Li recycling efficiency typically ranges from approximately 70 %–80 % [28–30]. Consequently, active materials in next-generation batteries, which may have lower concentrations of organic materials, could potentially raise concerns regarding the applicability of this recycling step. This is relevant, considering that research and current developments have placed neutral loading of Li as a primary method for the extraction of this valuable metal [28–30].

The results of the recycling process after neutral leaching are included in the Sankey diagrams for all the three systems studied in Fig. 6. Mass modelling was conducted on 100 batteries to facilitate balance analysis and visualisation of the resource potential.

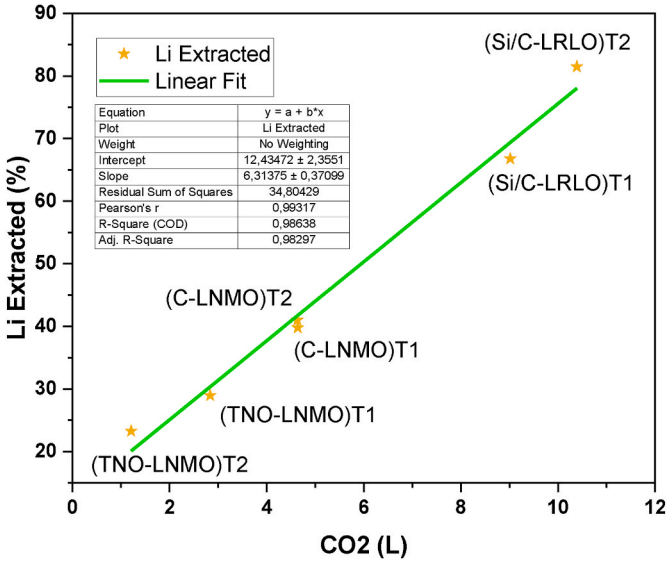

Fig. 5. Correlation between CO_2 emission during pyrolysis and Li recovery during neutral leaching (C-LNMO, TNO-LNMO, Si/C-LRLO).

The results indicated that during the pyrolysis stage, most of the organic compounds in the components were separated from the recycled materials and transformed into volatile matter. This out stream represent 16.6 wt%, 21.3 wt% and 13.9 wt% from the input material for the C-LNMO (Fig. 6a), TNO-LNMO (Fig. 6b), and Si/C-LRLO (Fig. 6c) systems.

After pyrolysis and mechanical treatment, the metallic components were segregated into a coarse fraction (>2 mm), called the metal fraction, primarily comprising Cu and Al foils alongside the casing material and a few fused particles. The brittleness of Cu and Al during pyrolysis, coupled with metal foil breakage during ball milling, resulted in the production of fine metal particles. Fig. 6 depicts a small portion of the metals (Cu and Al) embedded in the fine black mass, which was subsequently extractable through chemical methods.

Treatment of the C-LNMO and Si/C-LRLO systems resulted in the accumulation of metallic foils and casings comprising Al, Cu, and Fe. In contrast, the TNO-LNMO system accumulated only Al and Fe. From a metallurgical perspective, utilising Al alone as a current collector, as in the TNO-LNMO system, offers a higher recovery potential than mixed-material systems. Conversely, when the material fraction includes Cu, the separation of Al from Cu presents challenges and is economically unviable, leading to the expected loss of Al as a slag component during Cu recycling [74]. Fe does not pose a special challenge because it can be separated through magnetic separation and recycling proceeds in the Fe and steelmaking industries [75].

The neutral leaching process demonstrated efficient Li recovery for all three systems. Among them, Si/C-LRLO exhibited the highest Li recovery during neutral leaching compared with the C-LNMO and TNO-LNMO systems. As can be seen, the remaining Li in the delithiated black mass was later distributed in all subsequent products, with the main portion collected in the alkaline solution at the end of the hydrometallurgical recycling process. The Li extracted in neutral leaching and that found in the remaining alkaline solution are the only Li atoms accessible for extraction. Fig. 7a shows the total Li recovery efficiency and product distribution for these two key products. In general, it can be said that Li recovery was achieved up to 90 % in the Si/C-LRLO system, 80 % in the C-LNMO system, and 54 % in the TNO-LNMO system. It can also be observed that the selectivity of Li in neutral leaching was achieved, except for the TNO system, where only 55 % of the total extracted Li corresponded to that of neutral leaching. Here, it can be seen that, at least for the TNO-LNMO system using the same operating conditions, neutral leaching would not be fully advisable, unless the pyrolysis conditions were changed to reinforce lithium carbonisation, for instance, by blending the material with carbonaceous fractions or using a reducing gas during thermal operation.

As shown in Fig. 6, following neutral leaching, the delithiated black mass underwent acid leaching. This process generates leachate enriched with valuable metals, such as Ni and Mn, along with remaining traces of base metals, such as Cu, Al and Li. In contrast, elements resistant to sulfuric acid, which predominantly constitute the anode material, remained selectively as a solid product of acid leaching, representing the only stream in the recycling process. These materials contain small traces of contaminants, which vary from one battery type to another and are therefore referred in this study to as “crude” anode materials. As shown in Fig. 7b, the recovery efficiency of the anode material was selective and efficient. In the C-LNMO and Si/C-LRLO systems, approximately 78 % of the C was successfully recovered after acid leaching. In the Si/C-LRLO system, approximately 70 % of the Si was recovered along with carbon. In this particular case, Si does not dissolve in a weak concentration of sulfuric acid [76]. Based on the chemical composition of the "crude materials" analysed in the solid product, it was observed that among the metals, Al, Ni, and Mn appeared to have one of the highest concentration (1–2 wt%). This could have resulted from the leaching temperature and reduced acid concentration during the acid leaching process [77]. Notably, in the TNO-LNMO system, niobium (Nb) and titanium (Ti) were efficiently recovered at rates of approximately 90

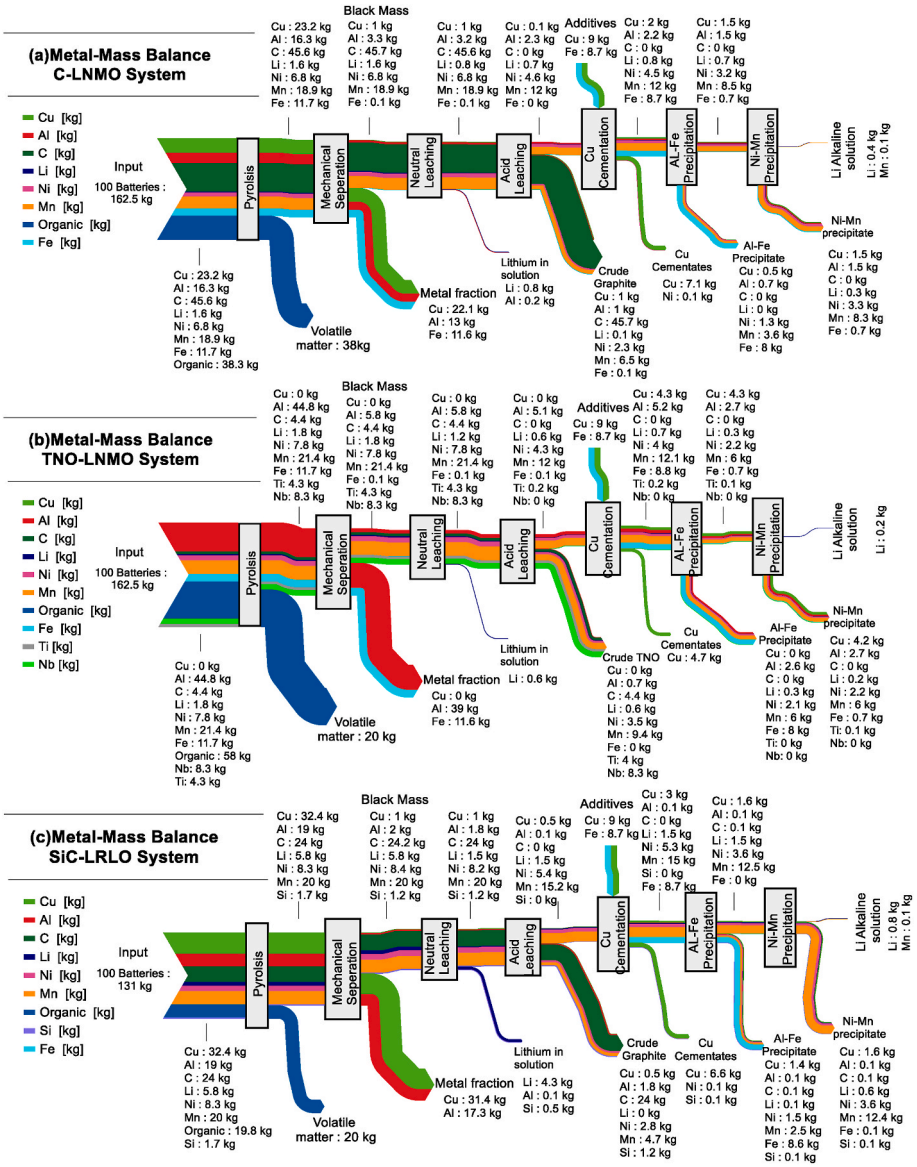

Fig. 6. Metal–mass balance of each processing step for all three systems, a. C-LNMO system, b. TNO-LNMO system and c. Si/C-LRLO system.

% and 65 %, respectively, while the carbon content resulting from the use of C65 was approximately 72 %. Based on these results, it can be concluded that such a product requires a refining process or the operation of the leaching process in a cascade structure. However, because of the limited availability of the material and because it was beyond the scope of this research, purification of the crude anode material was not included in this investigation.

The potential for further refinement of the anode materials through repeated acid leaching is viable. For crude graphite, the obtained product consisted of carbon-enriched graphite (91 % carbon) featuring minor Al traces and an absence of other metals, which is a favourable outcome relative to other systems. This material is of comparable quality to commercial raw graphite, with 55.2 % carbon and 1.7 % Al available in the market [79]. In the Si/C-LRLO system, graphite with silicon can be recycled for use in Si-C composite anodes, where a carbon content of more than 30 % is necessary [80]. The crude TNO recovered from TNO-LNMO can be thermally treated to transform it into a graphite-free material [81]. A brief overview of the transition of the anode material from post-pyrolysis through neutral and acid leaching based on the analysis of the solid products is provided in the supplementary material.

After separation of the anode material in the acid leaching process, the leachate first undergoes separation of the base metals as Cu-cementate and Al-Fe precipitates via cementation and alkaline precipitation, respectively. Based on the elemental flow shown in Fig. 6, these separation processes were highly selective with regard to Cu and Fe but were ineffective for Al, which remained in considerable amounts in the leachate solution, specifically in the C-LNMO and TNO-LNMO systems. The presence of Fe in the Cu cementate may indicate an excess of this element, which is more than needed to cement Cu in the solution. This is problematic because the Fe contamination in the cementate dissolves, requiring additional NaOH for the Al-Fe precipitation step. Despite impurities in the Cu-cementate (up to 9 wt% Fe and 0.2 wt% Al), it remains suitable for Cu recycling. During smelting, Fe and Al are oxidised and accumulate in the slag, whereas the recovered Cu is collected in the copper molten phase, metallurgically refined, cast as a copper anode in the recycling facility, and then electrolytically refined and sold as a cathode material [82]. Moreover, the addition of $CuSO_4$ should be re-evaluated in future research, as no evident positive effects were observed. In addition, future research should optimize pH to facilitate the removal of Al from the pregnant solution.

Regarding the quality of the products, the Al-Fe precipitate still contained a few impurities, such as Cu, Ni, and Mn, in all three systems.

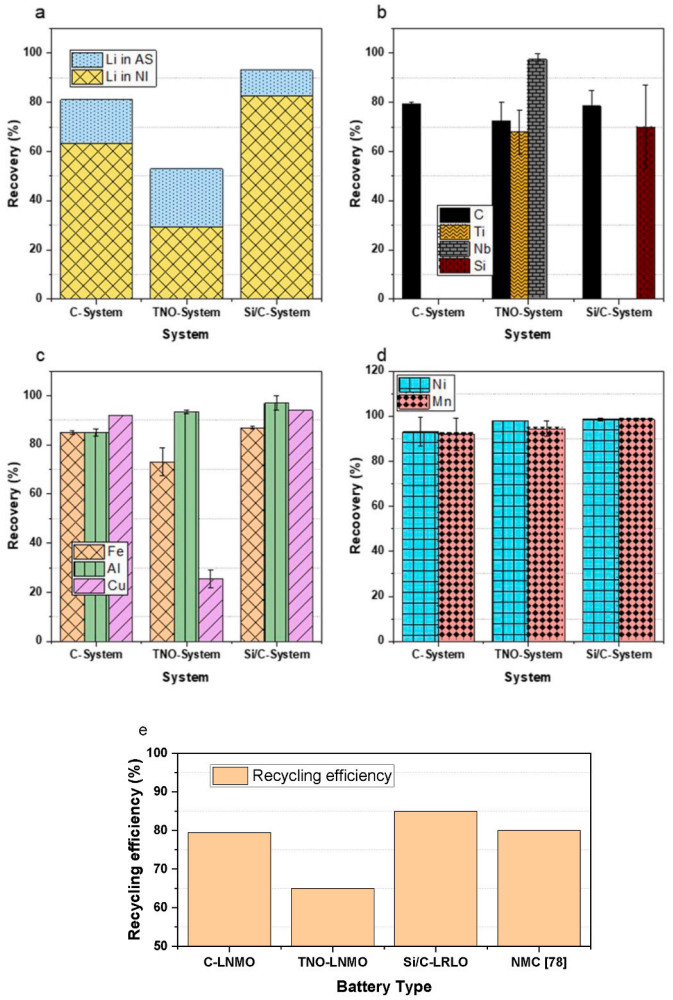

Fig. 7. Shows the metal recovery during precipitation: a. Li recovery, b. Anode material recovery, c. Cu-Fe-Al recovery, d. Ni-Mn recovery in all three systems, and e. Recycling efficiency compared to a commercial battery systems based on [78].

These should have precipitated in the previous step (for Cu) and subsequent steps (for Ni and Mn). Metal contamination could be attributed to the conservative selection of the pH value (3.3), which was chosen to prevent the precipitation of Ni and Mn. An Al-Fe filter cake containing valuable elements such as nickel could potentially be used as an input material in the Fe and steelmaking process as an alloying element for grade 3Ni4Al stainless steel, which requires a composition of 3 % Ni, remaining Fe, and other elements [83].

Moreover, the addition of $CuSO_4$ should be re-evaluated in future research, as no evident positive effect was observed. In addition, future research should optimize the pH to facilitate the removal of Al from the pregnant solution.

Metals such as Fe, Al, and Cu in LIBs are mostly in metallic form and mechanically separated during the recycling process. Therefore, as shown in Fig. 7c, the recovery efficiency still demonstrates outstanding performance, exceeding 80 % for Al in all three systems, averaging 80 % for Fe, and over 90 % for Cu. The only exception is the TNO-LNMO system, which does not use Cu as a current collector.

After the separation of the base metals, a Ni-Mn precipitation step was applied. Based on the elemental flow shown in Fig. 6, it can be stated that the separation of these valuable metals demonstrates outstanding performance in terms of selectivity for the targeted metals. However, this product shows significant contamination with undesired elements, such as Al and Cu. The situation with Li contamination is somewhat different because Li is not undesirable in cases where LNMO is produced. Nevertheless, the scope of this research did not allow the evaluation of the purification and regeneration of such materials. These findings provide opportunities for future research in this area.

As shown in Fig. 7d, the assessment of the recovery efficiency for Ni and Mn indicated outstanding performance. For both elements, efficiencies of 90 %, 95 %, and 97 % were registered for the C-LNMO, TNO-LNMO, and Si/C-LRLO systems, respectively.

4.3. Comparison of recycling process of the studied next generation cobalt-free with other commercial lithium-ion batteries

The assessment of the total recycling efficiency achieved using the defined recycling concept for all three evaluated systems is shown in Fig. 7e. As can be seen, the Si/C-LRLO system has the highest recycling efficiency at 85 %, followed by the C-LNMO and TNO-LNMO systems with approximately 80 % and 65 %, respectively. Fig. 7e also illustrates that, although this study provides only an initial overview of the recyclability of these new Co-free batteries, they already show competitive performance compared to the total recycling efficiency expected in the new regulation for 2025 and current reported data on commercial NMC batteries [78], highlighting the significant potential for optimisation. Little effort should be devoted to lithium recovery from the TNO-LNMO system to surpass the 2030 target of 70 %.

The recycling processes of cobalt-free lithium-ion batteries studied here reveal notable differences compared to those involving cobalt-containing batteries. The absence of cobalt simplifies the extraction of nickel and manganese by reducing the number of required reagents and steps, which can lead to lower overall costs and environmental impact. In addition, to a direct recovery of the anode material in all three studied cases. As shown in Fig. 7e, the recovery efficiency for lithium, nickel, and manganese in cobalt-free batteries is comparable to, or slightly different from, that in cobalt-containing batteries, reflecting both the advantages and limitations of the absence of cobalt. However, direct comparisons between cobalt-containing and cobalt-free battery recycling processes are limited, the elimination of cobalt is generally expected to reduce the need for complex chemical treatments and impurities.

Results compared with previous work on commercial cobalt-free batteries, such as LFP systems [53], indicated a lower Li yield recovery (99 %). However, Li et al. did not consider realistic conditions in the preprocessing stage, where both active materials are found together, as would be expected if the spent battery undergoes shredding and physical metal separation from the black mass. This study consider such a condition to evaluate the elemental dispersion through the hydrometallurgical processing. ther studies reported total recovery from LFP batteries with values ranging from 82 % to 90 which makes the recycling of the studied prototypes competitive with at least two of the three alternatives (C-LNMO and Si/C-LRLO systems) [84].

5. Conclusion

This study aims to advance the recycling practices for Co-free battery systems currently under development, focusing on systems that represent cutting-edge advancements in next-generation LIBs. The recyclability of the experimental cathode materials (TNO, Carbon, and Si/Carbon) and two types of electrolyte systems (ionic liquid and gelified) were evaluated using a recycling concept derived from literature and adapted to these modern prototypes. This study employed established hydrometallurgical techniques including pyrolysis, mechanical separation, neutral and acid leaching, cementation, and neutralisation with sodium hydroxide to achieve selective metal separation.

The findings indicated that gelified electrolytes demonstrated greater stability under pyrolysis than liquid electrolytes, which began to degrade at lower temperatures. This influenced the types and quantities of gases emitted, notably CO_2 and CO, which are crucial for the

subsequent stages of metal recovery. This includes a direct relationship between the CO_2 generated during pyrolysis and Li extracted via neutral leaching.

The ionic liquid electrolyte exhibited lower toxicity based on the PAC number, primarily because of reduced HF formation during pyrolysis. However, the study emphasised that all systems require stringent mitigation measures to control hazardous compounds, such as HF and PC, which pose significant environmental concerns.

The recycling processes were effective, complementing the outstanding performance of base metals, such as Cu, Al, and steel, which were separated through mechanical separation. Moreover, the recycling strategy succeeded in recovering valuable materials, particularly anode materials (graphite, Si/C, and TNO), Ni, Mn, and Li, with total recovery efficiencies ranging from 65 to 90 %. The recycling of metals surpassed the expected efficiencies within the upcoming regulation for 2025 and, with little optimisation of lithium recovery for the TNO-LNMO system, also reached competitive numbers by 2030.

Despite their excellent performance, challenges such as Al and Cu contamination in the anode material underscore the need for process optimisation and refining stages. In addition, it is necessary to improve thermal degradation to improve Li carbonisation during pyrolysis of the TNO-LNMO system. The results emphasise the importance of adjusting the pyrolysis conditions and acid leaching parameters to enhance the purity and overall yield of recycled materials.

The chemistry of the battery prototypes proved compatible with the recycling techniques used for commercial batteries, albeit with modifications to accommodate the unique characteristics of Co-free systems, especially for the TNO-LNMO system with gelified electrolyte. This compatibility is crucial for integrating new battery technologies into the existing recycling infrastructure. In this regard, besides the indications regarding electrolyte development, the results suggest that the new generation of batteries, which aim to reduce organic components—such as using a ceramic anode material like TNO—could impact current recycling technologies. Specifically, thermal treatment may not effectively produce Li-soluble compounds, thereby complicating the selective extraction of lithium during neutral leaching. However, acid-resistant materials like TNO, graphite and Si/C support the recovery and circularity of materials, facilitating the re-manufacturing of batteries. Future work should focus on the optimisation and study the viability of re-using the extracted purified anode material for battery manufacturing.

CRediT authorship contribution statement

Thanu Velmurugan: Writing – review & editing, Writing – original draft, Investigation, Formal analysis, Data curation, Conceptualization. **Fabian Diaz:** Writing – review & editing, Writing – original draft, Supervision, Conceptualization. **Lilian Schwich:** Supervision, Funding acquisition, Conceptualization. **Monika Keutmann:** Writing – review & editing, Supervision. **Bernd Friedrich:** Supervision, Funding acquisition, Conceptualization.

Declaration of competing interest

The authors declare that they have no known competing financial interests or personal relationships that could have appeared to influence the work reported in this paper.

Data availability

Data will be made available on request.

Acknowledgement

The authors would like to thank the collaborators and team members of the CoFBAT (G.A. No. 875126), and Si-DRIVE (G.A. No. 814464) projects for their contribution to the delivery and distribution of the tested materials. We are grateful for the financial support provided by the European Union's Horizon research and innovation programs. We also extend our thanks to the technical staff whose diligence and support were invaluable for the execution of this project.

Appendix A. Supplementary data

Supplementary data to this article can be found online at https://doi.org/10.1016/j.jpowsour.2024.235582.

References

[1] C. Padwal, H.D. Pham, S. Jadhav, T.T. Do, J. Nerkar, L.T.M. Hoang, A. Kumar Nanjundan, S.G. Mundree, D.P. Dubal, Deep eutectic solvents: green approach for cathode recycling of Li-ion batteries, Adv Energy and Sustain Res 3 (2022) 2100133, https://doi.org/10.1002/aesr.202100133.
[2] K. Yanamandra, D. Pinisetty, A. Daoud, N. Gupta, Recycling of Li-ion and lead acid batteries: a review, J. Indian Inst. Sci. 102 (2022) 281–295, https://doi.org/10.1007/s41745-021-00269-7.
[3] J. Neumann, M. Petranikova, M. Meeus, J.D. Gamarra, R. Younesi, M. Winter, S. Nowak, Recycling of lithium-ion batteries—current state of the art, circular economy, and next generation recycling, Adv. Energy Mater. 12 (2022) 2102917, https://doi.org/10.1002/aenm.202102917.
[4] A.M. Divakaran, M. Minakshi, P.A. Bahri, S. Paul, P. Kumari, A.M. Divakaran, K. N. Manjunatha, Rational design on materials for developing next generation lithium-ion secondary battery, Prog. Solid State Chem. 62 (2021) 100298, https://doi.org/10.1016/j.progsolidstchem.2020.100298.
[5] M.N. Akram, W.A. kader, EV Battery Recycling and its Impact on Society, vol. 3701, IEOM Society international, 2020. http://www.ieomsociety.org/detroit2020/papers/731.pdf.
[6] T. Georgi-Maschler, B. Friedrich, R. Weyhe, H. Heegn, M. Rutz, Development of a recycling process for Li-ion batteries, J. Power Sources 207 (2012) 173–182, https://doi.org/10.1016/j.jpowsour.2012.01.152.
[7] B.E. Murdock, K.E. Toghill, N. Tapia-Ruiz, A perspective on the sustainability of cathode materials used in lithium-ion batteries, Adv. Energy Mater. 11 (2021) 2102028, https://doi.org/10.1002/aenm.202102028.
[8] Critical Raw Materials Resilience: Charting a Path towards Greater Security and Sustainability, EUROPEAN COMMISSION, Critical Raw Materials Resilience: Charting a Path towards Greater Security and Sustainability, EUROPEAN COMMISSION: EUROPEAN COMMISSION, 2019.
[9] N. Muralidharan, R. Essehli, R.P. Hermann, R. Amin, C. Jafta, J. Zhang, J. Liu, Z. Du, H.M. Meyer, E. Self, J. Nanda, I. Belharouak, Lithium iron aluminum nickelate, LiNix fey alz O2 -new sustainable cathodes for next-generation cobalt-free Li-ion batteries, Adv. Mater. 32 (2020) e2002960, https://doi.org/10.1002/adma.202002960.
[10] X. Sun, Z. Liu, F. Zhao, H. Hao, Global competition in the lithium-ion battery supply chain: a novel perspective for criticality analysis, Environ. Sci. Technol. 55 (2021) 12180–12190, https://doi.org/10.1021/acs.est.1c03376.
[11] X. Sun, H. Hao, P. Hartmann, Z. Liu, F. Zhao, Supply risks of lithium-ion battery materials: an entire supply chain estimation, Mater. Today Energy 14 (2019) 100347, https://doi.org/10.1016/j.mtener.2019.100347.
[12] J. Nanda, V. Augustyn (Eds.), Transition Metal Oxides for Electrochemical Energy Storage, Wiley-VCH, Weinheim, 2022.
[13] C. Ekberg, M. Petranikova, Lithium batteries recycling, in: Lithium Process Chemistry, Elsevier, 2015, pp. 233–267.
[14] W. Li, S. Lee, A. Manthiram, High-nickel nma: a cobalt-free alternative to NMC and nca cathodes for lithium-ion batteries, Adv. Mater. 32 (2020) e2002718, https://doi.org/10.1002/adma.202002718.
[15] S.W.D. Gourley, T. Or, Z. Chen, Breaking free from cobalt reliance in lithium-ion batteries, iScience 23 (2020) 101505, https://doi.org/10.1016/j.isci.2020.101505.
[16] J.R. Croy, B.R. Long, M. Balasubramanian, A path toward cobalt-free lithium-ion cathodes, J. Power Sources 440 (2019) 227113, https://doi.org/10.1016/j.jpowsour.2019.227113.
[17] Y. Kim, W.M. Seong, A. Manthiram, Cobalt-free, high-nickel layered oxide cathodes for lithium-ion batteries: progress, challenges, and perspectives, Energy Storage Mater. 34 (2021) 250–259, https://doi.org/10.1016/j.ensm.2020.09.020.
[18] CoFBAT, D7.1 Study on possible recycling path including a flow sheet and mass balance. https://www.cofbat.eu/post/deliverable-7-1——study-on-possible-recycling-paths, 2021.
[19] K. Ryan, Silicon alloying anodes for high energy density batteries comprising lithium rich cathodes and safe ionic liquid based electrolytes for enhanced high VoltagE performance. Deliverable Report D8.6/D42 1st Si-DRIVE Workshop, 2020. https://sidrive2020.eu/about/.
[20] European Commission, Report from the Commission to the European Parliament, the Council, The European Economic And Social Committee And The Committee Of The Regions Brussels, 2019, 9.4.2019 COM 166.
[21] European Commission, Regulation of the European Parliament and of the Council, Com, 2020, p. 798.
[22] European Commission, Critical Raw Materials Resilience: Charting a Path towards Greater Security and Sustainability, COM, 2020, p. 474.
[23] J. Neumann, M. Petranikova, M. Meeus, J.D. Gamarra, R. Younesi, M. Winter, S. Nowak, Recycling of lithium-ion batteries—current state of the art, circular

economy, and next generation recycling, Adv. Energy Mater. 12 (2022) 2102917, https://doi.org/10.1002/aenm.202102917.
[24] S. Zhu, W. He, G. Li, X. Zhou, J. Huang, X. Zhang, Recovering copper from spent lithium ion battery by a mechanical separation process, in: 2011 International Conference on Materials for Renewable Energy & Environment, IEEE, Shanghai, China, 2011, pp. 1008–1012.
[25] J. Xiao, J. Li, Z. Xu, Recycling metals from lithium ion battery by mechanical separation and vacuum metallurgy, J. Hazard Mater. 338 (2017) 124–131, https://doi.org/10.1016/j.jhazmat.2017.05.024.
[26] G.D.J. Harper, E. Kendrick, P.A. Anderson, W. Mrozik, P. Christensen, S. Lambert, D. Greenwood, P.K. Das, M. Ahmeid, Z. Milojevic, W. Du, D.J.L. Brett, P. R. Shearing, A. Rastegarpanah, R. Stolkin, R. Sommerville, A. Zorin, J.L. Durham, A.P. Abbott, D. Thompson, N.D. Browning, B.L. Mehdi, M. Bahri, F. Schanider-Tontini, D. Nicholls, C. Stallmeister, B. Friedrich, M. Sommerfeld, L.L. Driscoll, A. Jarvis, E.C. Giles, P.R. Slater, V. Echavarri-Bravo, G. Maddalena, L.E. Horsfall, L. Gaines, Q. Dai, S.J. Jethwa, A.L. Lipson, G.A. Leeke, T. Cowell, J.G. Farthing, G. Mariani, A. Smith, Z. Iqbal, R. Golmohammadzadeh, L. Sweeney, V. Goodship, Z. Li, J. Edge, L. Lander, V.T. Nguyen, R.J.R. Elliot, O. Heidrich, M. Slattery, D. Reed, J. Ahuja, A. Cavoski, R. Lee, E. Driscoll, J. Baker, P. Littlewood, I. Styles, S. Mahanty, F. Boons, Roadmap for a sustainable circular economy in lithium-ion and future battery technologies, JPhys Energy 5 (2023) 21501, https://doi.org/10.1088/2515-7655/acaa57.
[27] M. Zhou, B. Li, J. Li, Z. Xu, Pyrometallurgical technology in the recycling of a spent lithium ion battery: evolution and the challenge, ACS EST Eng. 1 (2021) 1369–1382, https://doi.org/10.1021/acsestengg.1c00067.
[28] Y. Yao, M. Zhu, Z. Zhao, B. Tong, Y. Fan, Z. Hua, Hydrometallurgical processes for recycling spent lithium-ion batteries: a critical review, ACS Sustainable Chem. Eng. 6 (2018) 13611–13627, https://doi.org/10.1021/acssuschemeng.8b03545.
[29] H. Pinegar, Y.R. Smith, Recycling of end-of-life lithium-ion batteries, Part II: laboratory-scale research developments in mechanical, thermal, and leaching treatments, J. Sustain. Metall. 6 (2020) 142–160, https://doi.org/10.1007/s40831-020-00265-8.
[30] J. Xiao, J. Li, Z. Xu, Novel approach for in situ recovery of lithium carbonate from spent lithium ion batteries using vacuum metallurgy, Environ. Sci. Technol. 51 (2017) 11960–11966, https://doi.org/10.1021/acs.est.7b02561.
[31] L. Sun, K. Qiu, Organic oxalate as leachant and precipitant for the recovery of valuable metals from spent lithium-ion batteries, Waste Manag. 32 (2012) 1575–1582, https://doi.org/10.1016/j.wasman.2012.03.027.
[32] X. Zheng, Z. Zhu, X. Lin, Y. Zhang, Y. He, H. Cao, Z. Sun, A mini-review on metal recycling from spent lithium ion batteries, Engineering 4 (2018) 361–370, https://doi.org/10.1016/j.eng.2018.05.018.
[33] P. Meshram, A. Mishra, Abhilash, R. Sahu, Environmental impact of spent lithium ion batteries and green recycling perspectives by organic acids - a review, Chemosphere 242 (2020) 125291, https://doi.org/10.1016/j.chemosphere.2019.125291.
[34] H. Wang, B. Friedrich, Development of a highly efficient hydrometallurgical recycling process for automotive Li–ion batteries, J. Sustain. Metall. 1 (2015) 168–178, https://doi.org/10.1007/s40831-015-0016-6.
[35] C.-Y. Ku, J.-H. Chen, The recovery of lithium iron phosphate from lithium ion battery, in: 2022 8th International Conference on Applied System Innovation (ICASI), Nantou, Taiwan, IEEE, 2022, pp. 201–204.
[36] X. Chen, Y. Chen, T. Zhou, D. Liu, H. Hu, S. Fan, Hydrometallurgical recovery of metal values from sulfuric acid leaching liquor of spent lithium-ion batteries, Waste Manag. 38 (2015) 349–356, https://doi.org/10.1016/j.wasman.2014.12.023.
[37] S. Gu, L. Zhang, B. Fu, X. Wang, J.W. Ahn, Feasible route for the recovery of strategic metals from mixed lithium-ion batteries cathode materials by precipitation and carbonation, Chem. Eng. J. 420 (2021) 127561, https://doi.org/10.1016/j.cej.2020.127561.
[38] W. Liu, Q. Qin, H. Zhang, X. Chen, L. Luo, G. Li, S. Zheng, P. Li, Novel technology for the removal of Fe and Al from spent Li-ion battery leaching solutions by a precipitation–complexation process, ACS Sustainable Chem. Eng. 10 (2022) 13702–13709, https://doi.org/10.1021/acssuschemeng.2c03743.
[39] J. Hu, J. Zhang, H. Li, Y. Chen, C. Wang, A promising approach for the recovery of high value-added metals from spent lithium-ion batteries, J. Power Sources 351 (2017) 192–199, https://doi.org/10.1016/j.jpowsour.2017.03.093.
[40] J.C.-Y. Jung, P.-C. Sui, J. Zhang, A review of recycling spent lithium-ion battery cathode materials using hydrometallurgical treatments, J. Energy Storage 35 (2021) 102217, https://doi.org/10.1016/j.est.2020.102217.
[41] P. Liu, L. Xiao, Y. Tang, Y. Chen, L. Ye, Y. Zhu, Study on the reduction roasting of spent LiNixCoyMnzO2 lithium-ion battery cathode materials, J. Therm. Anal. Calorim. 136 (2019) 1323–1332, https://doi.org/10.1007/s10973-018-7732-7.
[42] D.P. Mantuano, G. Dorella, R.C.A. Elias, M.B. Mansur, Analysis of a hydrometallurgical route to recover base metals from spent rechargeable batteries by liquid–liquid extraction with Cyanex 272, J. Power Sources 159 (2006) 1510–1518, https://doi.org/10.1016/j.jpowsour.2005.12.056.
[43] J. Nan, D. Han, M. Yang, M. Cui, X. Hou, Recovery of metal values from a mixture of spent lithium-ion batteries and nickel-metal hydride batteries, Hydrometallurgy 84 (2006) 75–80, https://doi.org/10.1016/j.hydromet.2006.03.059.
[44] M. Joulié, R. Laucournet, E. Billy, Hydrometallurgical process for the recovery of high value metals from spent lithium nickel cobalt aluminum oxide based lithium-ion batteries, J. Power Sources 247 (2014) 551–555, https://doi.org/10.1016/j.jpowsour.2013.08.128.
[45] A. Jumari, M. Nizam, E.R. Dyartanti, Suranto, C.S. Yudha, S.U. Muzayanha, E. Apriliyani, A. Purwanto, A reductive pre-treatment to improve NCA cathode material hydrometallurgical recycle process, IOP Conf. Ser. Mater. Sci. Eng. 1096 (2021) 12135, https://doi.org/10.1088/1757-899X/1096/1/012135.
[46] S. Zhu, W. He, G. Li, X. Zhou, X. Zhang, J. Huang, Recovery of Co and Li from spent lithium-ion batteries by combination method of acid leaching and chemical precipitation, Trans. Nonferrous Metals Soc. China 22 (2012) 2274–2281, https://doi.org/10.1016/S1003-6326(11)61460-X.
[47] B. Swain, J. Jeong, J. Lee, G.-H. Lee, J.-S. Sohn, Hydrometallurgical process for recovery of cobalt from waste cathodic active material generated during manufacturing of lithium ion batteries, J. Power Sources 167 (2007) 536–544, https://doi.org/10.1016/j.jpowsour.2007.02.046.
[48] J. Kang, G. Senanayake, J. Sohn, S.M. Shin, Recovery of cobalt sulfate from spent lithium ion batteries by reductive leaching and solvent extraction with Cyanex 272, Hydrometallurgy 100 (2010) 168–171, https://doi.org/10.1016/j.hydromet.2009.10.010.
[49] S.M. Shin, N.H. Kim, J.S. Sohn, D.H. Yang, Y.H. Kim, Development of a metal recovery process from Li-ion battery wastes, Hydrometallurgy 79 (2005) 172–181, https://doi.org/10.1016/j.hydromet.2005.06.004.
[50] L. Sun, K. Qiu, Vacuum pyrolysis and hydrometallurgical process for the recovery of valuable metals from spent lithium-ion batteries, J. Hazard Mater. 194 (2011) 378–384, https://doi.org/10.1016/j.jhazmat.2011.07.114.
[51] W. Tang, X. Chen, T. Zhou, H. Duan, Y. Chen, J. Wang, Recovery of Ti and Li from spent lithium titanate cathodes by a hydrometallurgical process, Hydrometallurgy 147–148 (2014) 210–216, https://doi.org/10.1016/j.hydromet.2014.05.013.
[52] J. Li, X. Yang, Z. Yin, Recovery of manganese from sulfuric acid leaching liquor of spent lithium-ion batteries and synthesis of lithium ion-sieve, J. Environ. Chem. Eng. 6 (2018) 6407–6413, https://doi.org/10.1016/j.jece.2018.09.044.
[53] H. Li, S. Xing, Y. Liu, F. Li, H. Guo, G. Kuang, Recovery of lithium, iron, and phosphorus from spent LiFePO 4 batteries using stoichiometric sulfuric acid leaching system, ACS Sustainable Chem. Eng. 5 (2017) 8017–8024, https://doi.org/10.1021/acssuschemeng.7b01594.
[54] Y. Song, B. Xie, S. Song, S. Lei, W. Sun, R. Xu, Y. Yang, Regeneration of LiFePO 4 from spent lithium-ion batteries via a facile process featuring acid leaching and hydrothermal synthesis, Green Chem. 23 (2021) 3963–3971, https://doi.org/10.1039/D1GC00483B.
[55] Cofbat, Cobalt Free batteries. https://www.cofbat.eu/.
[56] Si-drive, Si-Based LIBS. https://sidrive2020.eu/.
[57] R.M. Lamya, L. Lorenzen, A Study of Factors Influencing the Kinetics of Copper Cementation during Atmospheric Leaching of Converter Matte, The Journal of The South African Institute of Mining and Metallurgy, 2005, pp. 21–28.
[58] F. Diaz, Y. Wang, R. Weyhe, B. Friedrich, Gas generation measurement and evaluation during mechanical processing and thermal treatment of spent Li-ion batteries, Waste Manag. 84 (2019) 102–111, https://doi.org/10.1016/j.wasman.2018.11.029.
[59] J. Zhang, A. Zhong, Z. Huang, D. Han, Experimental and kinetic study on the stabilities and gas generation of typical electrolyte solvent components under oxygen-lean oxidation and pyrolysis conditions, Sci. China Technol. Sci. 65 (2022) 2883–2894, https://doi.org/10.1007/s11431-022-2184-x.
[60] K. Liivand, M. Kazemi, P. Walke, V. Mikli, M. Uibu, D.D. Macdonald, I. Kruusenberg, Spent Li-ion battery graphite turned into valuable and active catalyst for electrochemical oxygen reduction, ChemSusChem 14 (2021) 1103–1111, https://doi.org/10.1002/cssc.202002742.
[61] H. Yang, X.-D. Shen, Dynamic TGA–FTIR studies on the thermal stability of lithium/graphite with electrolyte in lithium-ion cell, J. Power Sources 167 (2007) 515–519, https://doi.org/10.1016/j.jpowsour.2007.02.029.
[62] C. Rudolph, C.M. Grégoire, S.P. Cooper, S.A. Alturaifi, O. Mathieu, E.L. Petersen, B. Atakan, Spectroscopic study of CO formation from CO2-enriched pyrolysis of C2H6 and C3H8 under engine-relevant conditions, Applications in Energy and Combustion Science 14 (2023) 100123, https://doi.org/10.1016/j.jaecs.2023.100123.
[63] P.H. Cribb, J.E. Dove, S. Yamazakia, Kinetic study of the pyrolysis of methanol using shock tube and computer simulation techniques, Combust. Flame 88 (1992) 169–185, https://doi.org/10.1016/0010-2180(92)90050-Y.
[64] C. Rudolph, C.M. Grégoire, S.P. Cooper, S.A. Alturaifi, O. Mathieu, E.L. Petersen, B. Atakan, Spectroscopic study of CO formation from CO2-enriched pyrolysis of C2H6 and C3H8 under engine-relevant conditions, Applications in Energy and Combustion Science 14 (2023) 100123, https://doi.org/10.1016/j.jaecs.2023.100123.
[65] Rotzoll, High Temperature Pyrolysis Of Ethanol, J. Anal. Appl. Pyrol. 9 (1985) 43–52, https://doi.org/10.1016/0165-2370(85)80005-X.
[66] S. Balachandran, K. Forsberg, T. Lemaître, N. Vieceli, G. Lombardo, M. Petranikova, Comparative study for selective lithium recovery via chemical transformations during incineration and dynamic pyrolysis of EV Li-ion batteries, Metals 11 (2021) 1240, https://doi.org/10.3390/met11081240.
[67] G.S. Bhandari, N. Dhawan, Investigation of hydrogen reduction of LiCoO 2 cathode material for the recovery of Li and Co values, Energy Fuels 36 (2022) 15188–15198, https://doi.org/10.1021/acs.energyfuels.2c02871.
[68] J.B. DeLisio, X. Hu, T. Wu, G.C. Egan, G. Young, M.R. Zachariah, Probing the reaction mechanism of aluminum/poly(vinylidene fluoride) composites, J. Phys. Chem. B 120 (2016) 5534–5542, https://doi.org/10.1021/acs.jpcb.6b01100.
[69] Y. Ji, C.T. Jafvert, F. Zhao, Recovery of cathode materials from spent lithium-ion batteries using eutectic system of lithium compounds, Resour. Conserv. Recycl. 170 (2021) 105551, https://doi.org/10.1016/j.resconrec.2021.105551.
[70] E. F. Stephen/P. D. Miller, Solubility of Lithium Hydroxide in Water and Vapor Pressure of Solutions above 220° F, https://doi.org/10.1021/je60015a018.
[71] W.M. Haynes, CRC Handbook of Chemistry, 95th edition, 2014-2015.
[72] J. Jones, M. Anouti, M. Caillon-Caravanier, P. Willmann, D. Lemordant, Thermodynamic of LiF dissolution in alkylcarbonates and some of their mixtures

with water, Fluid Phase Equil. 285 (2009) 62–68, https://doi.org/10.1016/j.fluid.2009.07.020.
[73] M.T. Dunstan, F. Donat, A.H. Bork, C.P. Grey, C.R. Müller, CO2 capture at medium to high temperature using solid oxide-based sorbents: fundamental aspects, mechanistic insights, and recent advances, Chem. Rev. 121 (2021) 12681–12745, https://doi.org/10.1021/acs.chemrev.1c00100.
[74] M.A.T. Cocquerel, in: Aspects of Recycling Copper Scrap, Conservation & Recycling, vol. 2, 1978, pp. 111–116, https://doi.org/10.1016/0361-3658(78)90049-8, 2.
[75] W. Zhou, X. Liu, X. Lyu, W. Gao, H. Su, C. Li, Extraction and separation of copper and iron from copper smelting slag: a review, J. Clean. Prod. 368 (2022) 133095, https://doi.org/10.1016/j.jclepro.2022.133095.
[76] A.K. Panda, B.G. Mishra, D.K. Mishra, R.K. Singh, Effect of sulphuric acid treatment on the physico-chemical characteristics of kaolin clay, Colloids Surf. A Physicochem. Eng. Asp. 363 (2010) 98–104, https://doi.org/10.1016/j.colsurfa.2010.04.022.
[77] D.A. Ferreira, L.M.Z. Prados, D. Majuste, M.B. Mansur, Hydrometallurgical separation of aluminium, cobalt, copper and lithium from spent Li-ion batteries, J. Power Sources 187 (2009) 238–246, https://doi.org/10.1016/j.jpowsour.2008.10.077.
[78] M.d. Santos, I.A.A. Garde, C.M.B. Ronchini, L.C. Filho, G.B.M. de Souza, M.L. F. Abbade, N.N. Regone, V. Jegatheesan, J.A. de Oliveira, A technology for recycling lithium-ion batteries promoting the circular economy: the RecycLib, Resour. Conserv. Recycl. 175 (2021) 105863, https://doi.org/10.1016/j.resconrec.2021.105863.
[79] N.A. Laziz, J.A. Rjeily, A. Darwiche, J. Toufaily, A. Outzourhit, F. Ghamouss, M. T. Sougrati, Journal of Electrochemical Science and Technology 9 (4) (2018) 320–329, https://doi.org/10.5229/JECST.2018.9.4.320.hal-02065013.
[80] H.F. Andersen, J. Voje, Silicon - Carbon Composite Anode for Lithium - Ion Batteries, 2018. US 2018/0040880 A1.
[81] H. Pinegar, R. Marthi, P. Yang, Y.R. Smith, Reductive thermal treatment of LiCoO 2 from end-of-life lithium-ion batteries with hydrogen, ACS Sustainable Chem. Eng. 9 (2021) 7447–7453, https://doi.org/10.1021/acssuschemeng.0c08695.
[82] A. Khaliq, M. Rhamdhani, G. Brooks, S. Masood, Metal extraction processes for electronic waste and existing industrial routes: a review and Australian perspective, Resources 3 (2014) 152–179, https://doi.org/10.3390/resources3010152.
[83] R. Rahimi, B.C. de Cooman, H. Biermann, J. Mola, Microstructure and mechanical properties of Al-alloyed Fe–Cr–Ni–Mn–C stainless steels, Mater. Sci. Eng., A 618 (2014) 46–55, https://doi.org/10.1016/j.msea.2014.09.001.
[84] F. Forte, M. Pietrantonio, S. Pucciarmati, M. Puzone, D. Fontana, Lithium iron phosphate batteries recycling: an assessment of current status, Crit. Rev. Environ. Sci. Technol. 51 (2021) 2232–2259, https://doi.org/10.1080/10643389.2020.1776053.